Protective properties of new inhibitors based on substituted 1,2,4-thiadiazoles in hydrochloric acid solutions

A.D. Solovyev, M.D. Plotnikova* and A.B. Shein

Perm State National Research University, st. Bukireva 15, 614068 Perm, Russian Federation
**E-mail: plotnikova-md@mail.ru*

Abstract

The paper presents the results of a study of thiadiazole derivatives as corrosion inhibitors of mild steel in a solution of 1 M hydrochloric acid. 2-Amino-5-styryl-1,3,4-thiadiazole and 2-amino-5-heptyl-1,3,4-thiadiazole were studied. The semi-empirical GFN2-xTB Grimme method was used to calculate the protonation of the studied molecules in hydrochloric acid medium. Weight loss tests were carried out on C1018 steel at a temperature of 293 K, the exposure time of the samples was 24 h. The polarization curves in the temperature range of 293–353 K were recorded in the potentiodynamic mode in a three-electrode cell from the cathodic to the anodic potentials at a potential sweep rate of 0.5 mV/s, using a SOLARTRON 1280C electrochemical measuring complex. The case of the greatest inhibitory effect by the studied compounds was not distinguished, since at a concentration equal to or more than 100 mg/L, they all exhibit the same protective effect, taking into account the statistical error. A similar degree of protection of the metal surface by the studied inhibitors is associated with the same order of protonation of molecules in acidic solutions. Using the potentiodynamic polarization method, it was found that the studied compounds are inhibitors of the mixed (2-amino-5-styryl-1,3,4-thiadiazole) and cathodic (2-amino-5-heptyl-1,3,4-thiadiazole) types. The preservation of a high protective effect for inhibitors over the entire temperature range under study is associated with the process of chemical adsorption of inhibitor molecules on the metal surface, this fact is confirmed by the calculation of the activation energy of the corrosion process. The degrees of surface coverage of the steel with triazole molecules were calculated based on the results of electrochemical impedance spectroscopy at the corrosion potential. It was found that the adsorption process obeys the Freundlich equation for an energetically inhomogeneous surface. The results of this work point to the prospects of searching for potential inhibitors of acid corrosion in the series of thiadiazole derivatives.

Received: July 22, 2022. Published: September 15, 2022 doi: 10.17675/2305-6894-2022-11-3-27

Keywords: *mild steel, acid corrosion, thiadiazole, inhibitor, potentiodynamic polarization, activation energy, electrochemical impedance spectroscopy, adsorption.*

Introduction

Acid treatment is one of the most important stages in the development and enrichment of oil and gas wells [1–3]. The most common acidizing agents are hydrochloric, sulfuric, hydrofluoric, and phosphoric acids [4, 5]. However, in most acid treatments, HCl is used at a concentration of 1–5 M, since it forms soluble chlorides which is a significant advantage over other acids.

The action of acids must be suppressed by effective corrosion inhibitors to control corrosion of well tubulars, mixing tanks and other metal surfaces [6–8].

Organic compounds containing nitrogen, sulfur and oxygen atoms are the most known inhibitors. The influence of nitrogen-containing heterocyclic organic compounds on the corrosion of steel in acid solutions was studied by us earlier [9–11]. Other research groups have also proven that thiadiazole-type compounds are good corrosion inhibitors in aggressive environments [12–14].

It is known that most organic inhibitors act by adsorption to the metal surface. The adsorption of inhibitors is influenced by the nature and surface charge of the metal, the type of electrolyte used, and the chemical structure of the inhibitors with the charge of the molecules [15, 16].

In this work, we studied the inhibitory effect of two substituted 1,2,4-thiadiazoles with respect to C1018 structural steel in 1 M HCl solutions, taking into account the protonation of inhibitor molecules in the medium under study.

Experimental

Samples of mild steel C1018 with the composition, wt.%: Fe – 98.27; C – 0.20; Mn – 0.50; Si – 0.30; P – 0.04; S – 0.04; Cr – 0.15; Ni – 0.30; Cu – 0.20, were used in the study. The experiments were carried out in 1 M HCl solutions prepared from distilled water and 37% HCl. Organic synthesis products – triazole derivatives – were used as the corrosion inhibitors (Table 1).

Table 1. Inhibitors studied in the work.

Code	Formula	Name according to nomenclature
CP-4	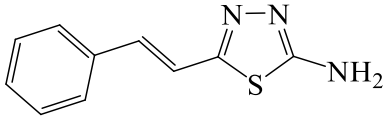	2-Amino-5-styryl-1,3,4-thiadiazole
CP-5	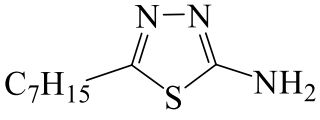	2-Amino-5-heptyl-1,3,4-thiadiazole

The presence of nitrogen atoms in the molecules of CP-20 and CP-38 inhibitors gives them basic properties in aqueous solutions. A semi-empirical calculation was performed

using the GFN2-xTB Grimm method [17, 18] to determine the protonation sequence of individual atoms taking implicit solvation in an aqueous medium into account.

The main parameters of C-steel corrosion were evaluated according to generally accepted methods [19]. Weight loss tests were carried out using rectangular plates made of C1018 steel with a size of 25×20×2 mm. The working surface area was 1180 mm^2.

The corrosion rates (*K* and *CR*), inhibition coefficient (γ) and degree of protection (Z_{wl}) were calculated using the equations:

$$K = \frac{m_0 - m}{S\tau}$$

$$CR = \frac{K}{\rho} \cdot 8.67$$

$$\gamma = \frac{K_0}{K}$$

$$Z_{wl} = \frac{K_0 - K}{K_0} \cdot 100\%$$

where m_0 is the mass of the initial sample, g; *m* is the mass of the sample after corrosion testing and removal of corrosion products, g; *S* is the surface area of the sample, m^2; τ is the immersion time, h; K_0 and *K* are the corrosion rates of steel in the pure solution and with addition of an inhibitor, respectively, in $g/(m^2 \cdot h)$.

A Solartron 1280C measuring complex (Great Britain) consisting of an impedance analyzer SI 1255 and a potentiostat SI 1287 and a three-electrode cell with separate cathodic and anodic spaces were used for electrochemical studies.

The polarization curves were recorded by the potentiodynamic technique from the cathodic to the anodic region at a scanning rate of 0.5 mV/s. All the potentials are presented in the silver chloride electrode scale.

Polarization measurements were carried out in the temperature range from 293 to 353 K. The cell was connected with a LOIP LT 100 thermostat with external circulation to maintain the required temperature.

Before each electrochemical experiment, the surface of the electrode was cleaned with sanding paper and then degreased with acetone.

The method of polarization curves allows one to calculate the corrosion rate (i_{corr}) in current density units, the corrosion potential (E_{corr}), and to determine the type of the inhibitor, *i.e.* which of the partial electrode reactions (hydrogen evolution or metal ionization) is mainly hindered by the inhibitor. This method also allows one to determine the Tafel sections of the polarization curves and calculate the degree of protection from electrochemical data [20]:

$$Z_{\text{wl}} = \frac{i_0 - i_{\text{inh}}}{i_0} \cdot 100\%$$

where i_0 and i_{inh} are the current densities of steel corrosion, respectively, in the pure solution and with addition of an inhibitor, in A/m^2.

Based on the electrochemical results the activation energy of the corrosion process was calculated. The calculations were performed by the temperature-kinetic method. The effect of temperature on the current density in cases of concentration polarization or delayed discharge stage is described by an equation similar to the Arrhenius equation [21]:

$$\ln i = -\frac{E_{\text{ef}}}{RT}$$

where i is the corrosion current density, A/m^2; E_{ef} is the effective activation energy of the corrosion process, J/mol; T is the temperature, K.

A straight line in the $\lg(i) = f(1/T)$ coordinates allows E_{ef}/R to be calculated as the slope.

The surface coverage (θ) of the C1018 electrode by corrosion inhibitor was determined from the equation:

$$\theta = \frac{C_0 - C}{C_0 - C_1}$$

where C_0, C and C_1 are, respectively, the capacitance of the double electric layer in the pure acid solution, in the solution with a given concentration of the inhibitors, and in the solution with $\theta = 1$. The value of C_1 was determined by extrapolating the curve in coordinates $C = f(1/C_{\text{inh}})$ to $(1/C_{\text{inh}}) = 0$, where C_{inh} is the concentration of the inhibitor in the solution, mg/L.

All the data presented in this work was obtained by averaging the results of three parallel measurements. MS Excel software was used to calculate the average results and standard deviations of direct and indirect measurements.

Results and Discussion

According to the results of quantum chemical calculations, the protonation of all inhibitors occurs predominantly at the nitrogen atoms of thiadiazole, with the N4 atom. The protonation of the amino group is disadvantageous both at the first and at the second step.

The optimal geometries of the neutral, mono-, and diprotonated forms of CP-4 and CP-5 inhibitors, the values of free energies, and the fractions of individual forms calculated from the Boltzmann distribution are shown in Figure 1 and Figure 2.

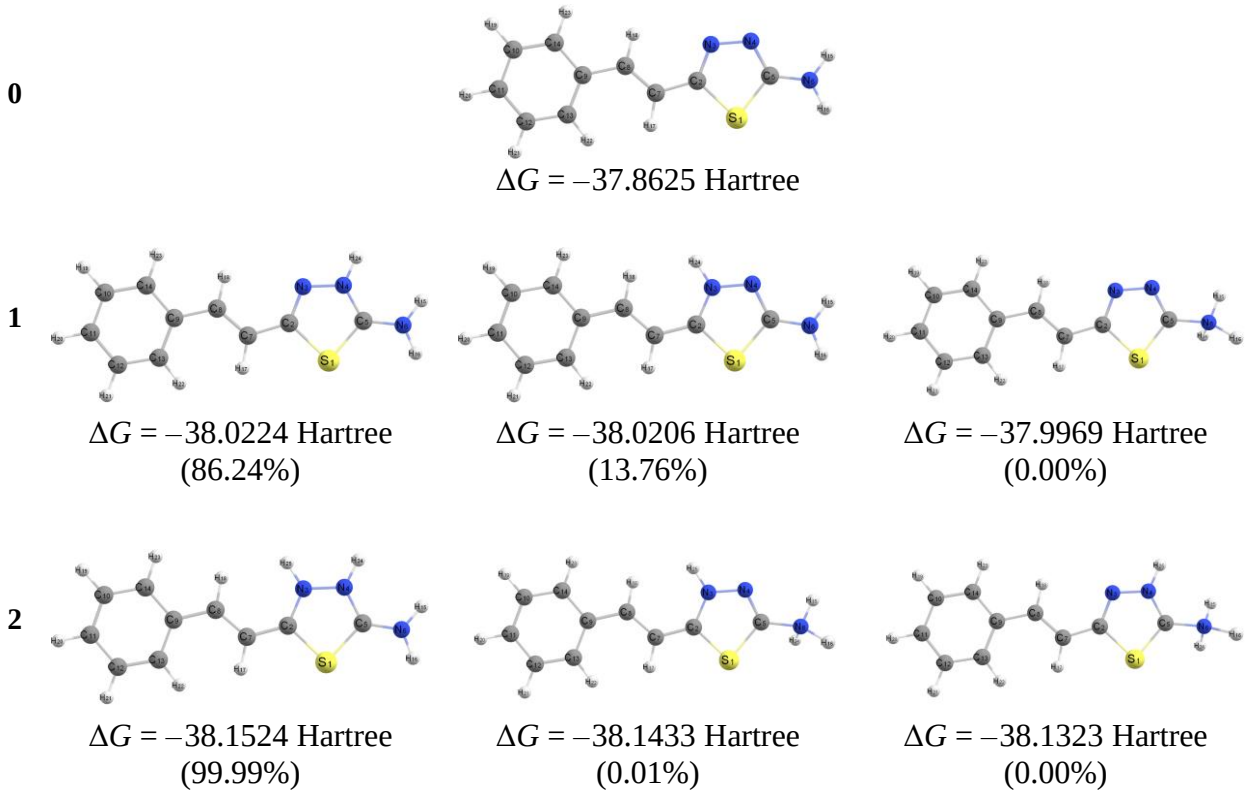

Figure 1. Structures optimized at the level of theory GFN2–xTB[GBSA(H_2O)] geometries of neutral CP-4 molecule and its protonated forms.

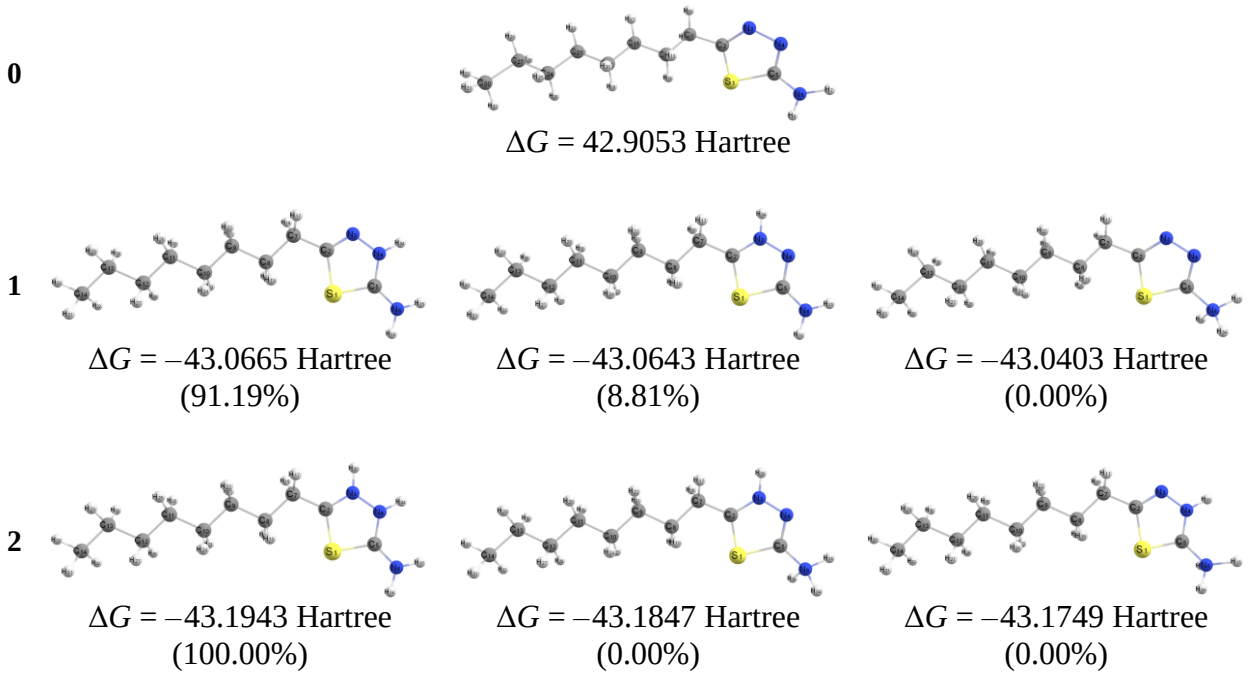

Figure 2. Structures optimized at the level of theory GFN2–xTB[GBSA(H_2O)] geometries of neutral CP-4 molecule and its protonated forms.

The results of weight loss tests of the studied compounds as corrosion inhibitors of structural steel C1018 in 1 M HCl solutions are presented in Table 2.

Table 2. Results of weight loss experiments on mild steel in solutions of 1 M hydrochloric acid in the presence of inhibitors.

Code	C_{inh}, mg/L	K, g/m^2·h	CR, mm/year	Z_{wl}, %	γ
–	–	2.51±0.13	2.78±0.14	–	–
CP-4	50	0.24±0.01	0.27±0.01	90.3±4.5	10.3±0.5
	100	0.24±0.01	0.26±0.01	90.6±4.3	10.6±0.5
	200	0.22±0.01	0.25±0.01	91.2±4.5	11.3±0.6
CP-5	50	0.49±0.02	0.54±0.03	80.6±4.0	5.2±0.3
	100	0.25±0.01	0.28±0.01	89.9±3.9	9.9±0.4
	200	0.23±0.01	0.26±0.01	90.7±3.9	10.7±0.4

Analyzing the presented results, we can say that the CP-5 inhibitor tends to increase the protective effect with increasing concentration, reaching maximum protective properties at concentrations equal to and above 100 mg/L. A satisfactory protective effect is achieved at an optimal concentration of 100 mg/L and further concentration of these solutions is unnecessary. The value of the adsorption of the inhibitor on the surface of the steel under study tends to the limit value even at a working solution concentration of 100 mg/L. The inhibitory effect of CP-4, in turn, practically does not change in the studied concentration range. This fact indicates that the adsorption equilibrium in the inhibitor solution – C1018 steel system is established at a solute concentration of 50 mg/L and does not shift when the solution is concentrated.

It is impossible to figure out the case of the greatest inhibitory effect of the studied compounds, since at a concentration equal to or more than 100 mg/L, they all exhibit the same protective effect, taking into account the statistical error (Table 2).

Comparing the results of weight loss studies and quantum chemical calculations, it can be assumed that a similar degree of protection of the metal surface by the studied inhibitors is associated with the same order of protonation of molecules in acidic solutions. The high protective properties at an initial concentration of CP-4 of 50 mg/L can be associated with the conjugation of the π-electrons of (2-phenyl)vinyl and the thiadiazole heterocycle through the alkene radical. Taking into account the structure of molecules (Table 1), we can say that the nonlinear hexyl radical of the CP-5 compound spatially hinders the adsorption of inhibitor molecules on the steel surface, which leads to saturation of the adsorption layer only at a concentration of 100 mg/L at the solid–liquid interface.

Figure 3 shows the polarization curves for steel C1018 in hydrochloric acid solutions without and with the addition of inhibitors of the thiadiazole series.

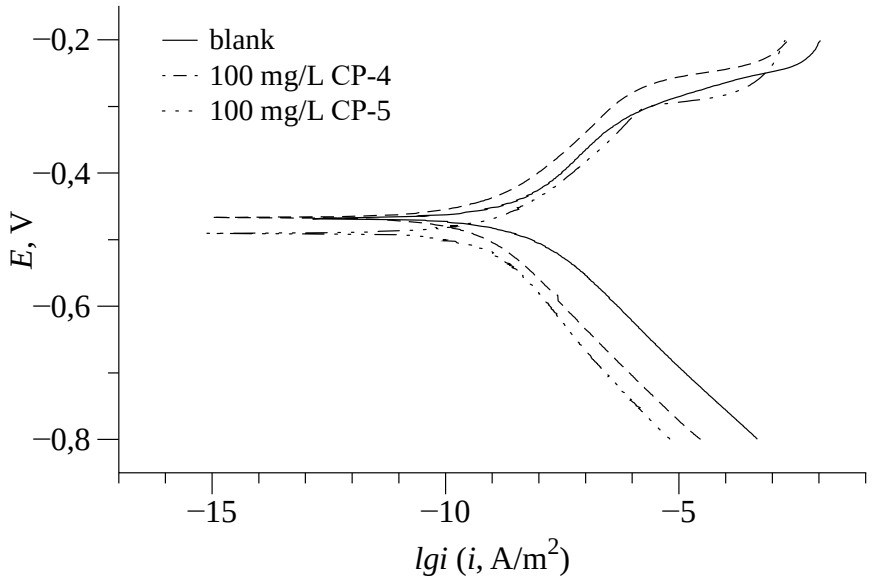

Figure 3. Polarization curves of C1018 steel in 1 M HCl containing 100 mg/L of the inhibitors at 293 K.

Table 3. Corrosion-electrochemical characteristics of C1018 in 1 M hydrochloric acid solutions with various concentrations with addition of 100 mg/L of the inhibitors at various temperatures.

Code	T, K	b_a, mV	b_c, mV	$i_{corr}\cdot10^5$, A/cm^2	$-E_{corr}$, V	Z_{wl}, %
	293	53±3	103±5	7.67±0.38	0.411±0.021	–
	303	65±2	92±3	8.00±0.24	0.432±0.013	–
–	313	65±3	84±3	8.34±0.33	0.439±0.018	–
	333	59±2	69±2	13.94±0.49	0.436±0.015	–
	353	44±2	81±4	52.75±2.89	0.417±0.021	–
	293	52±2	105±6	1.45±0.09	0.466±0.021	81.1±3.2
	303	65±3	90±3	1.87±0.11	0.494±0.022	76.6±2.9
CP-4	313	66±2	84±3	2.33±0.12	0.495±0.022	72.1±2.9
	333	69±3	65±3	3.91±0.20	0.496±0.019	72.0±2.4
	353	48±3	69±3	14.67±0.63	0.497±0.023	72.2±2.3
	293	54±3	103±5	1.90±0.11	0.464±0.026	75.2±2.6
	303	66±3	90±3	2.21±0.10	0.483±0.019	72.4±3.1
CP-5	313	62±3	86±3	2.30±0.19	0.473±0.019	72.4±2.7
	333	64±2	64±3	4.21±0.21	0.491±0.023	69.8±2.3
	353	49±2	73±2	14.32±0.67	0.477±0.014	72.9±2.6

The studied compound CP-4 has a greater effect on the cathodic partial electrochemical process [22, 23], however, the currents in the anode region also decrease, which classifies it as a mixed action inhibitor. The currents in the system with the addition of the CP-5 inhibitor fall in comparison with the currents in the initial acid solution only in the cathodic region, so it can be classified as a cathode-type inhibitor. The corrosion potential is shifted to the cathodic region only in the case of the CP-5 inhibitor.

The protective effect of the studied compounds was calculated (Table 3) based on the obtained polarization measurements.

Comparing the corrosion currents, it can be concluded that the corrosion rate increases with increasing temperature. Analyzing the functional dependences of the change in the protective effect on the temperature of the corrosion process, we can say that the preservation of a high protective effect for inhibitors over the entire temperature range under study is associated with the process of chemical adsorption of inhibitor molecules on the metal surface. According to the activation energy values presented in Table 4, the decrease in the values of E_a in the presence of CP-4 and CP-5 confirms the fact that the chemisorption process occurs on the steel surface [24, 25].

Table 4. The values of the activation energy of the corrosion process without and in the presence of inhibitors.

Code	*E*, kJ/mol
–	26.4±1.3
CP-4	3.9±0.2
CP-5	3.3±0.2

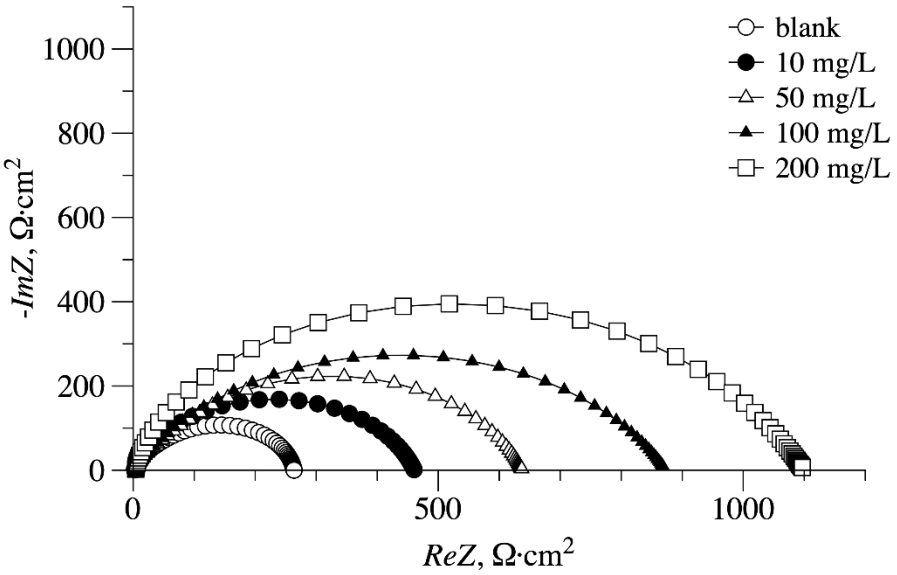

Figure 4. Impedance spectra of C1018 steel in a solution of 1 M HCl at E_{corr} with addition of various concentrations of CP-4.

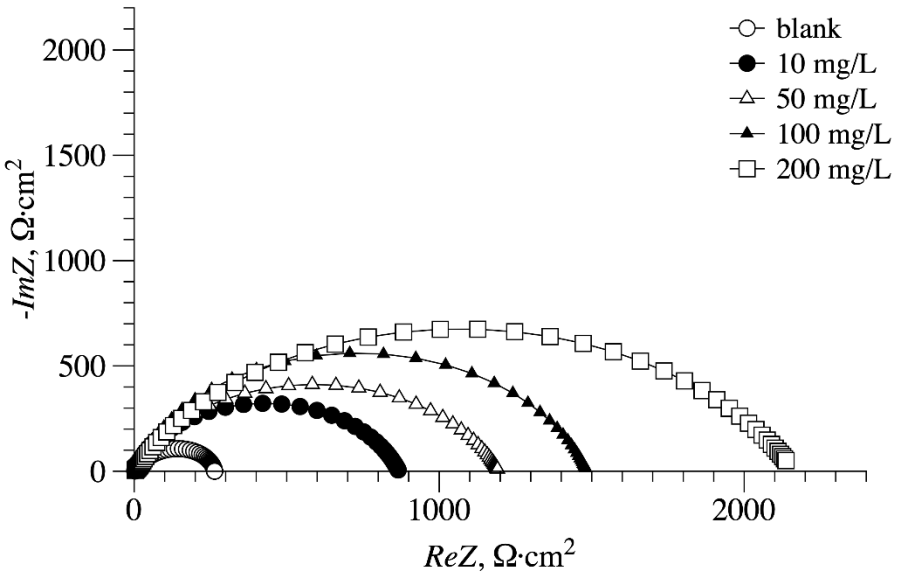

Figure 5. Impedance spectra of C1018 steel in a solution of 1 M HCl at E_{corr} with addition of various concentrations of CP-4.

The impedance spectra of C1018 steel in HCl solutions at the corrosion potential E_{corr} are a combination of semicircles of one capacitive arc in the high frequency region and an additional capacitive arc in solutions of CP-4 and CP-5. In Figures 4 and 5, ReZ is the real component of the impedance and $-ImZ$ is the imaginary component of the impedance.

The addition of the inhibitors to the system causes an increase in the diameter of the capacitive semicircle in the high frequency region, the greater the higher the inhibitor concentration, which is probably due to the hindrance of the electrode reactions.

The equivalent electrical circuit shown in Figure 6 was used to simulate the corrosion-electrochemical behavior of C1018 steel in a solution of 1 M HCl in the presence of CP-4 and CP-5 inhibitors. In this circuit: R_s is the solution resistance; R_1 is the resistance equal to $(R_a \cdot R_c)/(R_a + R_c)$, where R_a is the resistance of the anodic process (metal dissolution) and R_c is the resistance of the cathodic process (evolution of hydrogen); the resistance R_2 and the capacitance C_1 reflect the adsorption of an intermediate of the anodic process; CPE_1 is a constant phase element describing the capacitance of a double electric layer on an inhomogeneous surface of a solid electrode.

The values of the χ^2 parameter calculated in ZView2 for the circuits are in the range $(2–6)\cdot10^{-4}$, which indicates a good correlation with the experimental data.

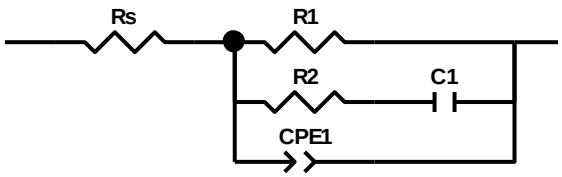

Figure 6. Equivalent electrical circuit for steel C1018 in 1 M HCl solution at E_{corr}.

The values of the parameters of the equivalent circuits (Figure 6) for the behavior of C1018 in an HCl solution in the presence of inhibitors are given in Table 5.

Table 5. Values of parameters of equivalent circuits for C1018 steel in 1 M HCl solution without and in the presence of inhibitors.

C_{inh}, mg/L	R_1, Ω·cm²	R_2, Ω·cm²	CPE_1, μF·cm^{-2}·s$^{(p-1)}$		C, μF/cm²	θ
			Q	p		
–	294±11	863±32	36.52±1.4	0.86±0.01	–	–
			CP-4			
10	459±16	532±21	73.88±2.2	0.80±0.01	1.41±0.07	0.96±0.01
50	637±19	745±27	56.75±1.7	0.76±0.01	2.40±0.09	0.97±0.01
100	871±24	961±36	44.07±1.5	0.77±0.01	2.77±0.09	0.98±0.01
200	1099±43	1366±49	35.51±1.4	0.75±0.01	2.84±0.08	0.98±0.01
			CP-5			
10	867±32	12±1	40.09±1.5	0.77±0.01	3.57±0.18	0.87±0.01
50	1195±46	50±3	35.95±1.3	0.74±0.01	1.53±0.08	0.91±0.01
100	1484±51	95±7	32.10±1.1	0.78±0.01	4.08±0.21	0.97±0.01
200	2164±67	135±9	20.20±0.9	0.79±0.01	1.25±0.6	0.98±0.01

It follows from Table 5 that there is a regular increase in the R_1 and R_2 resistances and a decrease in the Q parameter of the constant phase element CPE_1 (at comparable p values) with an increase in the concentration of the compounds studied. These correlations indicate the inhibition of the electrode processes (mainly the cathodic process) in the presence of the triazoles and their adsorption on the electrode surface. The R_2 and C_1 parameters, along with the interpretation of the adsorption of the intermediate of the cathodic process, can also be associated with the kinetics of the adsorption of compounds on the electrode surface (the Frumkin–Melik–Gaikazyan impedance without a diffusion impedance).

The degrees of surface coverage of the electrode with the inhibitor molecules are approximated in the coordinates of the Langmuir and Freundlich equations [26, 27] (Figure 7, Table 6).

The obtained values of the correlation coefficients indicate that the process of covering the surface with inhibitor molecules obeys to a greater extent the Freundlich isotherm, which describes adsorption on an energetically inhomogeneous surface. The high value of the adsorption constant in the presence of the CP-4 inhibitor suggests a greater adsorption of molecules on the C1018 surface, and hence a better ability to inhibit. This fact is confirmed by the results of electrochemical and gravimetric tests.

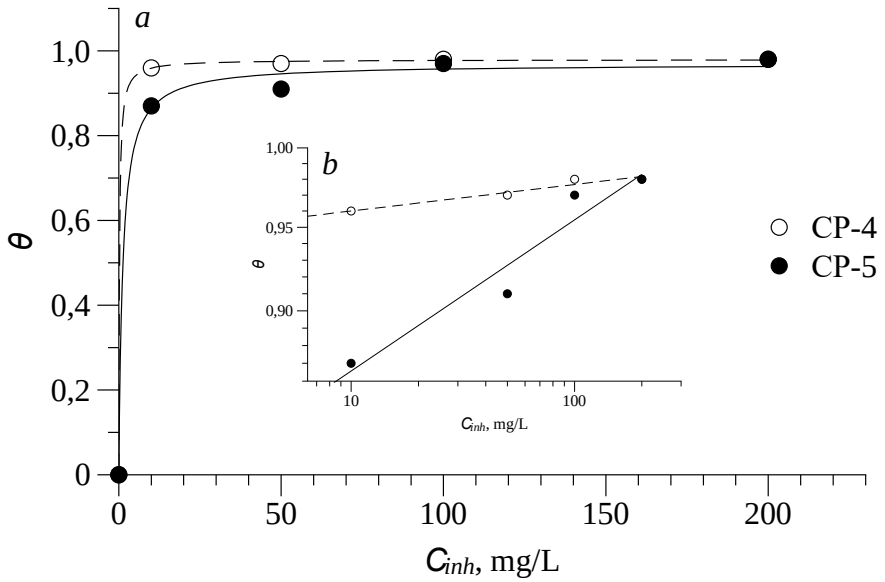

Figure 7. Langmuir (*a*) and Freundlich (*b*) isotherms of adsorption of inhibitors in 1 M HCl solutions.

Table 6. Parameters of Langmuir and Freundlich isotherms for the adsorption of CP-20 and CP-38 on the surface of C1018 in HCl solutions.

Code	Langmuir			Freundlich		
	K, dm³/g	Q, μmol/m²	R^2	K	n	R^2
CP-4	4.8037	0.9792	0.9999	0.9437	0.00074	0.9999
CP-5	0.8253	0.9688	0.9975	0.7850	0.0424	0.9992

Conclusions

1. Substituted 1,2,4-thiadiazoles presented in the work are effective inhibitors of acid corrosion of C1018 steel in 1 M HCl solution.
2. According to the results of quantum chemical calculations, the protonation of 2-amino-5-sitrile-1,3,4-thiadiazole and 2-amino-5-heptyl-1,3,4-thiadiazole proceeds predominantly at the nitrogen atoms of thiadiazole, with the first being protonated atom N4. The protonation of the amino group is disadvantageous neither at the first nor at the second step.
3. It is impossible to figure out the case of the greatest inhibitory effect of the studied compounds, since at a concentration equal to or more than 100 mg/L, they all exhibit the same protective effect, taking into account the statistical error. Comparing the results of weight loss studies and quantum chemical calculations, it can be assumed that a similar degree of protection of the metal surface by the studied inhibitors is associated with the same order of protonation of molecules in acidic solutions.

4. The decrease in the value of the activation energy in the presence of the studied nitrogen-containing heterocycles compared to 1 M HCl solution indicates that the adsorption process may be of a chemical nature. 2-amino-5-styryl-1,3,4-thiadiazole is a mixed type inhibitor, and 2-amino-5-heptyl-1,3,4-thiadiazole is cathodic. With an increase in temperature, the protective effect in the case of the studied inhibitors remains practically unchanged.
5. From the analysis of the impedance spectra, it follows that with an increase in the concentration of the inhibitor, the degree of coverage of the substrate surface by it increases, causing an increase in the protective effect.
6. The model of the Freundlich isotherm is typical to describe the processes of adsorption of the studied inhibitors on the surface of steel C1018.

Conflict of Interests

The authors declare there is no conflict of interests.

Acknowledgments

Funding: The research was supported by the Perm Research and Education Centre for Rational Use of Subsoil, 2022.

References

1. S.E. Roghayeh, A. Mehdi, M. Soraia, T. Milad, F. Hossein and R. Keyvan, Carboxamide derivatives as new corrosion inhibitors for mild steel protection in hydrochloric acid solution, *Corros. Sci*., 2019, **151**, 190–197. doi: 10.1016/j.corsci.2019.02.019
2. Yu.I. Kuznetsov, New possibilities of metal corrosion inhibition by organic heterocyclic compounds, *Int. J. Corros. Scale Inhib*., 2012, **1**, no. 1, 3–15. doi: 10.17675/2305-6894-2012-1-1-003-015
3. M.A. Deyab and Q. Mohsen, Inhibitory influence of cationic Gemini surfactant on the dissolution rate of N80 carbon steel in 15% HCl solution, *Sci. Rep*., 2021, **11**, 10521. doi: 10.1038/s41598-021-90031-x
4. T. Laabaissi, M. Rbaa, F. Benhiba, Z. Rouifi, U. Pramod Kumar, F. Bentiss, H. Oudda, B. Lakhrissi, I. Warad and A. Zarrouk, Insight into the corrosion inhibition of new benzodiazepine derivatives as highly efficient inhibitors for mild steel in 1 M HCl: Experimental and theoretical study, *Colloids Surf., A*, 2021, **629**, 127428. doi: 10.1016/j.colsurfa.2021.127428
5. A. Zarrouk, B. Hammouti, A. Dafali and F. Bentiss, Inhibitive properties and adsorption of purpald as a corrosion inhibitor for copper in nitric acid medium, *Ind. Eng. Chem. Res*., 2013, **52**, 2560–2568. doi: 10.1021/ie301465k

6. Y. Qiang, S. Zhang and L. Wang, Understanding the adsorption and anticorrosive mechanism of DNA inhibitor for copper in sulfuric acid, *Appl. Surf. Sci*., 2019, **492**, 228–238. doi: 10.1016/j.apsusc.2019.06.190
7. X. Li, S. Deng, H. Fu and T. Li, Adsorption and inhibition effect of 6-benzylaminopurine on cold rolled steel in 1.0 M HCl, *Electrochim. Acta*, 2009, **54**, 4089–4098. doi: 10.1016/j.electacta.2009.02.084
8. Yu.I. Kuznetsov and L.P. Kazansky, Physicochemical aspects of metal protection by azoles as corrosion inhibitors, *Russ. Chem. Rev*., 2008, **77**, no. 3, 219–232. doi: 10.1070/RC2008v077n03ABEH003753
9. M.D. Plotnikova, A.B. Shein, M.G. Shcherban' and A.D. Solovyev, The study of thiadiazole derivatives as potential corrosion inhibitors of low-carbon steel in hydrochloric acid, *Bulletin of the University of Karaganda – Chemistry*, 2021, **103**, no. 3, 93–102. doi: 10.31489/2021Ch3/93-102
10. M.D. Plotnikova, A.D. Solovyev, A.B. Shein, A.N. Bakiev and A.S. Sofronov, New inhibitors based on substituted 1,2,4-triazoles for mild steel in hydrochloric acid solutions, *Int. J. Corros. Scale Inhib*., 2021, **10**, no. 3, 1230–1244. doi: 10.17675/2305-6894-2021-10-3-23
11. M.D. Plotnikova, A.D. Solovyev, A.B. Shein, A.N. Vasyanin and A.S. Sofronov, Corrosion inhibition of mild steel by triazole and thiadiazole derivatives in 5 M hydrochloric acid medium, *Int. J. Corros. Scale Inhib*., 2021, **10**, no. 3, 1336–1354. doi: 10.17675/2305-6894-2021-10-3-29
12. Y. Boughoues, M. Benamira, L. Messaadia and N. Ribouh, Adsorption and corrosion inhibition performance of some environmental friendly organic inhibitors for mild steel in HCl solution *via* experimental and theoretical study, *Colloids Surf., A*, 2020, **593**, 124610. doi: 10.1016/j.colsurfa.2020.124610
13. M.H.O. Ahmed, A.A. Al-Amiery, Y.K. Al-Majedy, A.A.H. Kadhum, A.B. Mohamad and T.S. Gaaz, Synthesis and characterization of a novel organic corrosion inhibitor for mild steel in 1 M hydrochloric acid, *Results Phys*., 2018, **8**, 728–733. doi: 10.1016/j.rinp.2017.12.039
14. K.F. Khaled, Experimental and molecular dynamics study on the inhibition performance of some nitrogen containing compounds for iron corrosion, *Mater. Chem. Phys*., 2010, **124**, 760–767. doi: 10.1016/j.matchemphys.2010.07.055
15. K.F. Khaled, Molecular simulation, quantum chemical calculations and electrochemical studies for inhibition of mild steel by triazoles, *Electrochim. Acta*, 2008, **53**, 3484–3492. doi: 10.1016/j.electacta.2007.12.030
16. G. Lei, O. Ime Bassey, Z. Xingwen, S. Xun, Q. Yujie, K. Savas and K. Cemal, Theoretical insight into an empirical rule about organic corrosion inhibitors containing nitrogen, oxygen, and sulfur atoms, *Appl. Surf. Sci*., 2017, **406**, 301–306. doi: 10.1016/j.apsusc.2017.02.134

17. C. Bannwarth, E. Caldeweyher, S. Ehlert, A. Hansen, P. Pracht, J. Seibert, S. Spicher and S. Grimme, Extended tight-binding quantum chemistry methods, *WIREs Computational Molecular Science*, 2021, **11**, e1493. doi: 10.1002/wcms.1493
18. C. Bannwarth, S. Ehlert and S. Grimme, GFN2-xTB – An Accurate and Broadly Parametrized Self-Consistent Tight-Binding Quantum Chemical Method with Multipole Electrostatics and Density-Dependent Dispersion Contributions, *J. Chem. Theory Comput*., 2019, **15**, 1652–1671. doi: 10.1021/acs.jctc.8b01176
19. L. Liang, C. Ting-Ting, Z. Qi-Wei and C. Chong-Wei, Organic Phosphorus Compounds as Inhibitors of Corrosion of Carbon Steel in Circulating Cooling Water: Weight Loss Method and Thermodynamic and Quantum Chemical Studies, *Adv. Mater. Sci. Eng*., 2018, 1653484. doi: 10.1155/2018/1653484
20. F. Mansfeld, Tafel slopes and corrosion rates obtained in the pre-Tafel region of polarisation curves, *Corros. Sci*., 2005, **47**, no. 12, 3178–3186. doi: 10.1016/j.corsci.2005.04.012
21. P. Dohare, K. Ansari, M. Quraishi and I. Obot, Pyranpyrazole derivatives as novel corrosion inhibitors for mild steel useful for industrial pickling process: experimental and quantum chemical study, *J. Ind. Eng. Chem*., 2017, **52**, 197–210. doi: 10.1016/j.jiec.2017.03.044
22. O. Devos, C. Gabrielli and B. Tribollet, Simultaneous EIS and in situ microscope observation on a partially blocked electrode application to scale electrodeposition, *Electrochim. Acta*, 2006, **51**, 1413–1422. doi: 10.1016/j.electacta.2005.02.117
23. T. Bochuan, Z. Shengtao, Q. Yujie, G. Lei, F. Li, L. Chaohui, X. Yue and C. Shijin, A combined experimental and theoretical study of the inhibition effect of three disulfide-based flavouring agents for copper corrosion in 0.5 M sulfuric acid, *J. Colloid Interface Sci*., 2018, **526**, 268–280. doi: 10.1016/j.jcis.2018.04.092
24. R. Solmaz, Investigation of adsorption and corrosion inhibition of mild steel in hydrochloric acid solution by 5-(4-Dimethylaminobenzylidene)rhodanine, *Corros. Sci*., 2014, **79**, 169–176. doi: 10.1016/j.corsci.2013.11.001
25. K.R. Ansari, M.A. Quraishi and A. Singh, Schiff's base of pyridyl substituted triazoles as new and effective corrosion inhibitors for mild steel in hydrochloric acid solution, *Corros. Sci*., 2014, **79**, 5–15. doi: 10.1016/j.corsci.2013.10.009
26. T.D. Batueva, M.G. Shcherban' and N.B. Kondrashova, Mesoporous silica materials and their sorption capacity for tungsten (VI) and molybdenum (VI) ions, *Inorg. Mater*., 2019, **55**, 1146–1150. doi: 10.1134/S0020168519110013
27. S.A. Umoren, I.B. Obot, A.U. Israel, P.O. Asuquo, M.M. Solomon, U.M. Eduok and A.P. Udoh, Inhibition of mild steel corrosion in acidic medium using coconut coir dust extracted from water and methanol as solvents, *J. Ind. Eng. Chem. (Washington, D. C.)*, 2014, **20**, 3612–3622. doi: 10.1016/j.jiec.2013.12.056

♦ ♦ ♦